Robust Adaptive Prescribed Performance Control of Motor Servo System with Input Dead-zone

Zhenle Dong, Dongjie Bai, Yizhuang Duan, Siyuan Pan, Shuai Wang, Geqiang Li

Abstract—**For the issue of tracking control of motor servo system with input dead-zone, a novel robust adaptive prescribed performance control is proposed. Firstly, a smooth dead-zone inverse model is introduced and parameterized, which can help compensate for dead-zone. Secondly, the prescribed performance function is used to constrain the convergence process of tracking error. Then, a robust adaptive controller is designed based on the estimation of the upper bound of disturbance to weaken the influence from disturbance. Comparative tracking verification under two position command cases is carried out and the simulation results show that the proposed controller can improve the tracking accuracy well.**

Index Terms—**motor servo system, input dead-zone, disturbance, prescribed performance, asymptotic stability**

I. INTRODUCTION

MOTOR servo systems have been widely used in industrial and defense fields, such as electric machine tool [1], load simulator [2], and launch turntable [3], etc. Developing high-precision controller is the key to improve the performance. However, controller design always faces many challenges, including modelling uncertainties, disturbance, input nonlinearity, etc., and these problems are also hot research topics at home and abroad in recent years.

How to deal with disturbance has always been a hot issue in nonlinear control, and the existing methods include disturbance observer [4], sliding mode control [5], RISE control [6], neural network control [7], [8], fuzzy control [9], [10], and so on. Input dead-zone is a typical input nonlinearity and the methods to deal with this issue mainly include two categories. One is to regard input dead-zone as the combination of smooth input and disturbance, then adopt appropriate disturbance suppression technique to weaken its effect, such as [11]. The disadvantage of this method is that it leads to oversize lumped disturbance and may face the risk of high gain robust feedback which may cause system instability. The other method is to model dead-zone specifically, and then compensate its effect based on the inverse model of dead-zone. The second method is more targeted and has been applied in many fields [12], [13].

However, the above researches only focus on the steady-state performance. For many applications of motor servo system, transient performance (such as overshoot and convergence speed) is also the key to reliable operation. Therefore, controller design needs to pay attention to both transient performance and steady-state performance. For transient performance, [14] proposed the prescribed performance control, which can achieve settable transient performance and steady-state performance by designing a performance function to constrain the tracking error. This method has been applied in many fields [15], [16], [17].

For steady-state performance, the most ideal theoretical control result is asymptotic stability, that is, the tracking error can approach zero as time goes on. Through the investigation of the existing researches, it was found that for motor servo system with input dead-zone, the controller that comprehensively considers prescribed performance and steady-state asymptotic tracking to improve the tracking accuracy as much as possible has not been studied, which become the inspiration of this research.

The paper is organized as follows: In Part II, a nonlinear mathematical model of motor servo system with unknown input dead-zone is built, and a smooth dead-zone inverse model is introduced to transform the system model into the format that facilitates the compensation of unknown dead-zone. In Part III, the robust adaptive controller with prescribed performance and asymptotic tracking is designed. In Part IV, the performance that can be achieved by the proposed controllers is given through the rigorous Lyapunov analysis. Finally, the effectiveness of the proposed controller is verified through the comparison of four chosen controllers.

II. MATHEMATICAL MODELING

The working principle of the considered motor servo system with input dead-zone is shown in Fig.1. The servo driver controls the motor to drive the load to rotate, and the control input acts on the system after passing through the dead-zone.

Manuscript received April 11, 2024; revised July 22, 2024.

This work was supported in part by Natural Science Foundation of China under Grant 52305056, in part by Henan Province Science and Technology Research Projects under Grant 242102220009, 242102220026.

Zhenle Dong is an associate professor at the School of Vehicle and Transportation Engineering, Henan University of Science and Technology. Luoyang 471000, China (Corresponding author, e-mail: dong_zhenle@163.com).

Dongjie Bai is a postgraduate student at the School of Vehicle and Transportation Engineering, Henan University of Science and Technology. Luoyang 471000, China (e-mail: b18339631260@163.com).

Yizhuang Duan is a postgraduate student at the School of Vehicle and Transportation Engineering, Henan University of Science and Technology. Luoyang 471000, China (e-mail: duanyizhuang306@163. com).

Siyuan Pan is an assistant experimentalist at the School of Business, Henan University of Science and Technology. Luoyang 471000, China (e-mail: 499017141@qq.com)

Shuai Wang is a lecturer at the School of Mechatronics Engineering, Henan University of Science and Technology. Luoyang 471000, China (e-mail: wang5451140@163.com).

Geqiang Li is a professor at the School of Mechatronics Engineering, Henan University of Science and Technology. Luoyang 471000, China (e-mail: hitligeqiang@163.com).

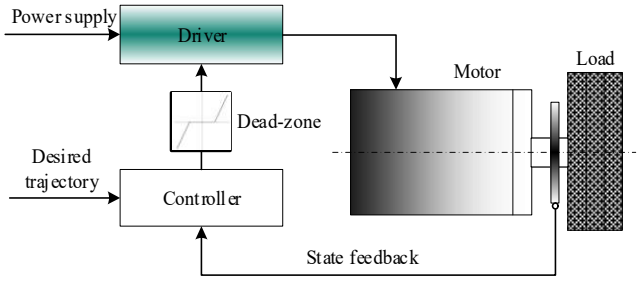

Fig. 1. Structure diagram of motor servo system with input dead-zone

The load dynamic equation is

$$J\ddot{y} = k_u g(u) - B\dot{y} + d(t) \tag{1}$$

where J is the load inertia, y, $\dot{y}$, $\ddot{y}$ are the position, velocity and acceleration respectively, k_u is the voltage-torque gain, B is unknown and denotes the effective viscous friction coefficient, $d(t)$ is modeling uncertainty, u is the control input, $g(u)$ is the dead-zone function and can be represented as

$$g(u) = \begin{cases} m_1 u - m_1 b_1 & \text{if } u \ge b_1 \\ 0 & \text{if } b_2 < u < b_1 \\ m_2 u - m_2 b_2 & \text{if } u \le b_2 \end{cases} \tag{2}$$

where $m_1 > 0$, $m_2 > 0$, $b_1 \ge 0$, $b_2 \le 0$ denote the right slope, left slope, right break-point and left break-point of the dead-zone respectively and these parameters are unknown constants.

The curve of dead-zone function given in (2) is [13]

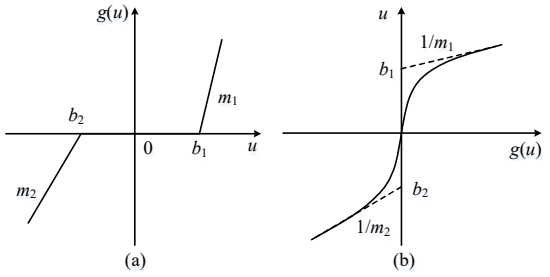

Fig. 2 Dead-zone and its smooth inverse

To compensate the dead-zone, we introduce the smooth dead-zone inverse and its curve is shown in Fig. 2(b) [13]. It should be noted that the curves in Fig. 2 are all redrawn based on the properties of the equation (2)(3)(4).

Define $I(\bullet)$ as the inverse dead-zone model, i.e.,

$$u = I(g) = \frac{g + m_1 b_1}{m_1}\xi_1(g) + \frac{g + m_2 b_2}{m_2}\xi_2(g) \tag{3}$$

where $\xi_1(\bullet)$ and $\xi_2(\bullet)$ are smooth functions defined as

$$\xi_1(\bullet) = \frac{e^{\bullet/\kappa}}{e^{\bullet/\kappa} + e^{-\bullet/\kappa}} \quad , \quad \xi_2(\bullet) = \frac{e^{-\bullet/\kappa}}{e^{\bullet/\kappa} + e^{-\bullet/\kappa}} \tag{4}$$

where $\kappa > 0$ is an adjustable parameter.

Define $\boldsymbol{\vartheta} = [\vartheta_1, \vartheta_2, \vartheta_3, \vartheta_4]^T$ as the unknown dead-zone parameter vector, and $\vartheta_1 = m_1$, $\vartheta_2 = m_1 b_1$, $\vartheta_3 = m_2$, $\vartheta_4 = m_2 b_2$, then model (2) can be rewritten as

$$g = -\boldsymbol{\vartheta}^T \boldsymbol{\chi} \tag{5}$$

where $\boldsymbol{\chi} = [-\zeta_+ u, \zeta_+, -\zeta_- u, \zeta_-]^T$, and ζ_+, ζ_- are defined as

$$\zeta_+ = \begin{cases} 1, & \text{if } g > 0 \\ 0, & \text{else} \end{cases} \quad , \quad \zeta_- = \begin{cases} 1, & \text{if } g < 0 \\ 0, & \text{else} \end{cases} \tag{6}$$

Noting that ζ_+ and ζ_- are discontinuous, which may cause inconvenience to controller design, we define

$$g_d = -\hat{\boldsymbol{\vartheta}}^T \hat{\boldsymbol{\chi}} \tag{7}$$

where $\hat{\boldsymbol{\vartheta}} = [\hat{\vartheta}_1, \hat{\vartheta}_2, \hat{\vartheta}_3, \hat{\vartheta}_4]^T$ is the estimation of $\boldsymbol{\vartheta}$, $\boldsymbol{\chi} = [-\xi_1(u)u, \xi_1(u), -\xi_2(u)u, \xi_2(u)]^T$.

Then we have

$$g - g_d = -\boldsymbol{\vartheta}^T \boldsymbol{\chi} + \hat{\boldsymbol{\vartheta}}^T \hat{\boldsymbol{\chi}} = \tilde{\boldsymbol{\vartheta}}^T \hat{\boldsymbol{\chi}} + \boldsymbol{\vartheta}^T (\hat{\boldsymbol{\chi}} - \boldsymbol{\chi}) \tag{8}$$

where $\tilde{\boldsymbol{\vartheta}} = \hat{\boldsymbol{\vartheta}} - \boldsymbol{\vartheta}$ is the estimation error.

Substituting (8) into (1), we have

$$\frac{J}{k_u}\ddot{y} = g_d - \frac{B}{k_u}\dot{y} + \tilde{\boldsymbol{\vartheta}}^T \frac{\hat{\boldsymbol{\chi}}}{k_u} + D(t) \tag{9}$$

where

$$D(t) = d(t)/k_u + \boldsymbol{\vartheta}^T(\hat{\boldsymbol{\chi}} - \boldsymbol{\chi})/k_u$$

By defining the state vector $\boldsymbol{x} = [x_1, x_2]^T = [y, \dot{y}]^T$, we can obtain the state-space-equation of the considered system as

$$\begin{aligned} \dot{x}_1 &= x_2 \\ \frac{J}{k_u}\dot{x}_2 &= g_d - \theta\dot{y} + \tilde{\boldsymbol{\vartheta}}^T \frac{\hat{\boldsymbol{\chi}}}{k_u} + D(t) \end{aligned} \tag{10}$$

where $\theta = B/k_u$.

Assumption 1: The upper bound of disturbance $D(t)$ exists but is unknown, i.e., $D(t) \le \kappa$, and κ denotes an unknown constant.

The control object can be described as: Given the desired trajectory $y_d = x_{1d}$, design a control input u to make the position y track y_d as accurately as possible with input dead-zone.

III. Controller Design

Define the tracking error as $e_m = x_1 - x_{1d}$ and set the following error constraint

$$-\underline{\eta}\delta(t) < e_m(t) < \overline{\eta}\delta(t) \ , \forall t > 0 \tag{11}$$

where $\underline{\eta}, \overline{\eta}$ are positive adjustable parameters, $\delta(t) > 0$ is a smooth decreasing function defined as

$$\delta(t) = (\delta_0 - \delta_\infty)e^{-kt} + \delta_\infty \ , \ \lim_{t\to\infty}\delta(t) = \delta_\infty > 0 \tag{12}$$

where δ_0, δ_∞, k are positive adjustable parameters. Obviously, formula (11) (12) can impose prescribed performance (overshoot, convergence speed, and steady-state threshold) on tracking error e_m.

Further, we define the following increasing function

$$\begin{aligned} &-\underline{\eta} < P(z_1) < \overline{\eta}, \forall t > 0 \\ &\lim_{z_1\to+\infty} P(z_1) = \overline{\eta} \ , \ \lim_{z_1\to-\infty} P(z_1) = -\underline{\eta} \end{aligned} \tag{13}$$

where z_1 denotes the transformed error, and it is easy to check that $e_m(t) = \delta(t)P(z_1)$ and formula (13) will hold provided that z_1 is bounded.

A usable form of $P(z_1)$ is [14]

$$P(z_1) = \frac{\overline{\eta}e^{z_1} - \underline{\eta}e^{-z_1}}{e^{z_1} + e^{-z_1}} = \frac{e_m(t)}{\delta(t)} = \beta \tag{14}$$

Finding the inverse function of (14), we have

$$z_1 = \frac{1}{2}\ln\frac{\beta + \underline{\eta}}{\overline{\eta} - \beta} \tag{15}$$

then we will design the final controller based on z_1.

Taking the derivative of (15), we have

$$\begin{aligned}\dot{z}_1 &= \frac{1}{2}\frac{\overline{\eta}+\underline{\eta}}{(r+\underline{\eta})(\overline{\eta}-r)}\cdot\dot{\beta} \\ &= \gamma(\dot{e}_{\mathrm{m}} - e_{\mathrm{m}}\dot{\delta}/\delta) = \gamma(x_2 - \dot{x}_{1\mathrm{d}} - e_{\mathrm{m}}\dot{\delta}/\delta)\end{aligned} \tag{16}$$

where $\gamma = (\overline{\eta}+\underline{\eta})/[2\delta(\beta+\underline{\eta})(\overline{\eta}-\beta)]$.

Define $z_2 = \dot{z}_1 + k_1 z_1$, where $k_1 > 0$ is an adjustable parameter. With the state-space-equation (10), we have

$$\begin{aligned}\frac{J}{k_{\mathrm{u}}}\dot{z}_2 = \frac{J}{k_{\mathrm{u}}}\dot{\gamma}(x_2 - \dot{x}_{1\mathrm{d}} - e_{\mathrm{m}}\dot{\delta}/\delta) + \frac{J}{k_{\mathrm{u}}}\gamma[-\ddot{x}_{1\mathrm{d}} - (\dot{e}_{\mathrm{m}}\dot{\delta}\delta + \\ e_{\mathrm{m}}\ddot{\delta}\delta - e_{\mathrm{m}}\dot{\delta}^2)/\delta^2] + \gamma[g_{\mathrm{d}} - \theta\dot{y} + \tilde{\boldsymbol{\vartheta}}^{\mathrm{T}}\frac{\hat{\boldsymbol{\chi}}}{k_{\mathrm{u}}} + D(t)] + \frac{Jk_1\dot{z}_1}{k_{\mathrm{u}}}\end{aligned} \tag{17}$$

then g_{d} can be designed as

$$\begin{aligned}&g_{\mathrm{d}} = g_{\mathrm{m}} + g_{\mathrm{r1}} + g_{\mathrm{r2}} \\ &g_{\mathrm{m}} = (\frac{J}{k_{\mathrm{u}}}f_1 + \hat{\theta}\dot{y}\gamma)/\gamma \ , \ g_{\mathrm{r1}} = -k_2 z_2/\gamma \ , \\ &g_{\mathrm{r2}} = -\frac{k_{\mathrm{r}} z_2 \hat{\kappa}^2}{k_{\mathrm{r}} z_2 \tanh[z_2/\omega(t)]\hat{\kappa} + \omega(t)} \\ &f_1 = -\dot{\gamma}(x_2 - \dot{x}_{1\mathrm{d}} - e_{\mathrm{m}}\dot{\delta}/\delta) - \gamma[-\ddot{x}_{1\mathrm{d}} - (\dot{e}_{\mathrm{m}}\dot{\delta}\delta \\ &\quad + e_{\mathrm{m}}\ddot{\delta}\delta - e_{\mathrm{m}}\dot{\delta}^2)/\delta^2] - k_1\dot{z}_1 \\ &\dot{\hat{\theta}} = -k_\theta z_2 \dot{y}\gamma \ , \ \dot{\hat{\kappa}} = k_D\gamma|z_2|\end{aligned} \tag{18}$$

where g_{m} is the model-based compensation term containing the prescribed performance constraint given in (11)(12), g_{r1} is the linear stabilizing term, g_{r2} is the nonlinear robust term to suppress the disturbance $D(t)$ [18], $\hat{\theta}$ is the estimation of θ, $\hat{\kappa}$ is the estimation of κ, $\omega(t) > 0$ is an indicator function to be designed, and k_2, k_{r}, k_θ, k_D are adjustable parameters.

Substituting (18) into (17), it we have

$$\frac{J}{k_{\mathrm{u}}}\dot{z}_2 = -k_2 z_2 + \gamma g_{\mathrm{r2}} + \tilde{\theta}\dot{y} + \tilde{\boldsymbol{\vartheta}}^{\mathrm{T}}\frac{\tilde{\boldsymbol{\chi}}\gamma}{k_{\mathrm{u}}} + \gamma D(t) \tag{19}$$

where $\tilde{\theta} = \hat{\theta} - \theta$ is the estimation error.

Then the final control input can be designed as

$$\begin{aligned}&u = DI(g_{\mathrm{d}}) = \frac{g_{\mathrm{d}} + \hat{\vartheta}_2}{\hat{\vartheta}_1}\psi_1(g_{\mathrm{d}}) + \frac{g_{\mathrm{d}} + \hat{\vartheta}_4}{\hat{\vartheta}_3}\psi_2(g_{\mathrm{d}}) \\ &\dot{\hat{\boldsymbol{\vartheta}}} = -\boldsymbol{\Gamma}_{\boldsymbol{\vartheta}} z_2 \tilde{\boldsymbol{\chi}}\gamma/k_{\mathrm{u}}\end{aligned} \tag{20}$$

where $\boldsymbol{\Gamma}_{\boldsymbol{\vartheta}}$ is an adjustable parameter matrix.

The schematic diagram of the proposed controller is shown in Fig. 3.

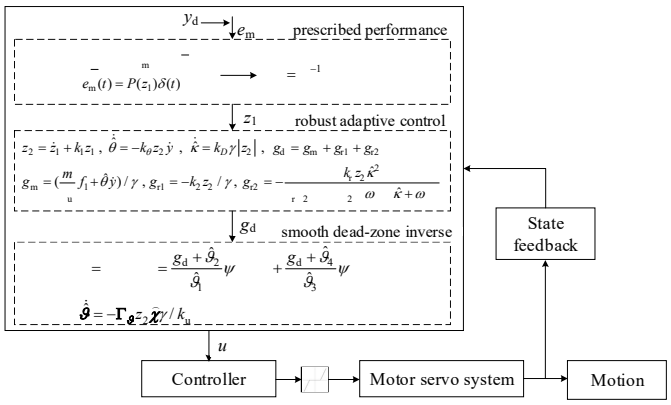

Fig. 3. Schematic diagram of the proposed controller

IV. Main Results

If the initial tracking error $e_{\mathrm{m}}(0)$ satisfies $-\underline{\eta}\delta(0) < e_{\mathrm{m}}(0) < \overline{\eta}\delta(0)$, and the indicator function $\omega(t)$ satisfies $\int_0^t \gamma\omega(t)d\tau < \overline{\omega}$ where $\overline{\omega}$ is positive constant, the proposed controller (18)(20) can realize that

1) All the signals of the closed-loop motor servo system are bounded, and the prescribed performance given in (11)(12) can always be satisfied.

2) By properly choosing controller parameters, asymptotic stability can be obtained, i.e., $e_{\mathrm{m}} \to 0$, as $t \to \infty$.

Proof of 1):

Define the following Lyapunov function

$$V = \frac{J}{2k_{\mathrm{u}}}z_2^2 + \frac{1}{2k_\theta}\tilde{\theta}^2 + \frac{1}{2}\tilde{\boldsymbol{\vartheta}}^{\mathrm{T}}\boldsymbol{\Gamma}_{\boldsymbol{\vartheta}}^{-1}\tilde{\boldsymbol{\vartheta}} + \frac{1}{2k_D}\tilde{\kappa}^2 \tag{21}$$

where $\tilde{\kappa} = \hat{\kappa} - \kappa$ is the estimation error.

Taking the derivative of V, and substituting (18)(20), we have

$$\begin{aligned}\dot{V} &= z_2\frac{J}{k_{\mathrm{u}}}\dot{z}_2 + \frac{1}{k_\theta}\tilde{\theta}\dot{\hat{\theta}} + \tilde{\boldsymbol{\vartheta}}^{\mathrm{T}}\boldsymbol{\Gamma}_{\boldsymbol{\vartheta}}^{-1}\dot{\hat{\boldsymbol{\vartheta}}} + \frac{1}{k_D}\tilde{\kappa}\dot{\hat{\kappa}} \\ &= -k_2 z_2^2 + z_2\gamma g_{\mathrm{r2}} + z_2\tilde{\theta}\dot{y} + z_2\tilde{\boldsymbol{\vartheta}}^{\mathrm{T}}\hat{\boldsymbol{\chi}}\gamma + z_2\gamma D(t) \\ &\quad + \frac{1}{k_\theta}\tilde{\theta}\dot{\hat{\theta}} + \tilde{\boldsymbol{\vartheta}}^{\mathrm{T}}\boldsymbol{\Gamma}_{\boldsymbol{\vartheta}}^{-1}\dot{\hat{\boldsymbol{\vartheta}}} + \tilde{\kappa}\gamma|z_2| \\ &\le -k_2 z_2^2 - \frac{\gamma k_{\mathrm{r}} z_2^2 \hat{\kappa}^2}{k_{\mathrm{r}} z_2 \tanh[z_2/\omega(t)]\hat{\kappa} + \omega(t)} + \hat{\kappa}\gamma|z_2|\end{aligned} \tag{22}$$

With the property $0 \le x\tanh(x/a) \le x$, $x \in R$, $a > 0$, we can further obtain

$$\begin{aligned}\dot{V} &\le -k_2 z_2^2 - \frac{\gamma k_{\mathrm{r}} z_2^2 \hat{\kappa}^2}{k_{\mathrm{r}}|z_2|\hat{\kappa} + \omega(t)} + \hat{\kappa}\gamma|z_2| \\ &\le -k_2 z_2^2 + \frac{\hat{\kappa}\gamma|z_2|\omega(t)}{k_{\mathrm{r}}|z_2|\hat{\kappa} + \omega(t)} \le -k_2 z_2^2 + \frac{\gamma\omega(t)}{k_{\mathrm{r}}}\end{aligned} \tag{23}$$

Integrating the two side of inequality (23), we have

$$V + \int_0^t k_2 z_2^2 d\tau \le V(0) + \int_0^t \frac{\gamma\omega(t)}{k_{\mathrm{r}}}d\tau \le V(0) + \frac{\overline{\omega}}{k_{\mathrm{r}}} \tag{24}$$

Because the initial states are bounded, from (24), we know that V and z_2 are bounded. From (21), it is easy to check that $\tilde{\theta}, \tilde{\boldsymbol{\vartheta}}, \tilde{\kappa}$ are bounded, that is, $\hat{\theta}, \hat{\boldsymbol{\vartheta}}, \hat{\kappa}$ are bounded. For that the transfer function between z_1 and z_2 is stable, then z_1 is bounded. Then from (15), we known that $\beta \in (-\underline{\eta}, \overline{\eta})$, so tracking error e_{m} could always satisfy the prescribed performance given in (11)(12).

From the expression of γ, it not hard to see that γ is positive and bounded by $(\underline{\eta}+\overline{\eta})/(\delta_\infty\underline{\eta}\overline{\eta})$, then it is easy to check that g_{m} and g_{r1} are bounded. For g_{r2}, with the property $|x| \le x\tanh(x/a) + \eta a$, $x \in R$, $a > 0$, η=0.2785, we have

$$\begin{aligned}|g_{\mathrm{r2}}| &\le k_{\mathrm{r}}\hat{\kappa}^2\frac{|z_2|}{k_{\mathrm{r}} z_2 \tanh[z_2/\omega_1(t)]\hat{\kappa} + \omega(t)} \\ &\le k_{\mathrm{r}}\hat{\kappa}^2\frac{z_2\tanh[z_2/\omega(t)] + \gamma\omega(t)}{k_{\mathrm{r}} z_2 \tanh[z_2/\omega(t)]\hat{\kappa} + \omega(t)} \\ &\le \hat{\kappa} + \gamma k_{\mathrm{r}}\hat{\kappa}^2\end{aligned} \tag{25}$$

so g_{r2} is bounded, then we know g_{d} and final control input u are bounded.

Proof of 2):

From (24), we have $z_2 \in L_2$. From (19), we have $\dot{z}_2 \in L_\infty$, i.e., z_2 is uniformly continuous. By Barbalat's lemma [19], we have $t \to \infty$, $z_2 \to 0$, then we have $t \to \infty$, $z_1 \to 0$. Based on the definition in (15), it can be found that $\beta \to (\overline{\eta} - \underline{\eta})/2$. Obviously that if parameters $\underline{\eta}$ and $\overline{\eta}$ are set equal, β will approach zero, the tracking error e_m will approach zero, then the asymptotic stability can be realized, i.e., $e_m \to 0$ as $t \to \infty$. This completes the proof.

V. VERIFICATION

The parameters of the considered motor servo system are shown in Table 1.

TABLE I
PARAMETERS OF MOTOR SERVO SYSTEM

Symbol	Value	Symbol	Value
J	$0.01kg{\cdot}m^2$	$m_1 = m_2$	1
k_u	$5N{\cdot}m/V$	b_1	$0.1V$
B	$1.025N{\cdot}m$	b_2	$-0.1V$

In order to verify the effectiveness of the proposed controller, the following four controllers are chosen for comparison.

(1) C1: This is the proposed controller and the detailed expressions are in (18)(20). By trill-and-error, the controller parameters are selected as: $k_1 = 2$, $k_2 = 2$, $\varepsilon = 0.2$, k_r = 1e-5, $k_D = 1$, $\omega(t) = 1000/[\gamma(t^2+0.1)]$, $k_\theta = 0.002$, Γ_ϑ = diag(1e-2, 1e-7).

(2) C2: This is the robust adaptive prescribed performance controller. Compared to C1, the dead-zone compensation is removed in C2. The control input and the actual valid input are considered to be equal, i.e. $u = g_d$. To ensure that the comparison is valid, the controller parameters are equal to the corresponding parameters of C1.

(3) C3: This is the adaptive prescribed performance controller. Compared to C2, this controller does not contain the nonlinear robustness term g_{r2}. To ensure that the comparison is valid, the controller parameters are taken to be the same as the corresponding parameters of C1.

(4) C4: Compared to C3, this controller removes the prescribed performance constraint, i.e., the controller is designed not based on error z_1, but the tracking error e_m. The controller is structured as

$$\begin{aligned} e_2 &= \dot{e}_m + k_1 e_m \,, \\ u &= \hat{\theta} x_2 - k_2 e_2 + \frac{m}{k_u}(\ddot{x}_{1d} + k_1 \dot{e}_m) \,, \\ \dot{\hat{\theta}} &= -k_\theta e_2 x_2 \end{aligned} \tag{26}$$

To ensure that the comparison is valid, the controller parameters are taken to be the same as the corresponding parameters of C1.

Case 1：

The desired position trajectory is chosen as x_{1d} = arctan(sin(0.5πt)) (1-exp (-0.01t^3)) rad and shown in Fig. 4. The simulation step size is set as 0.0005s. The simulation results are shown in Fig. 4-6 and Table II.

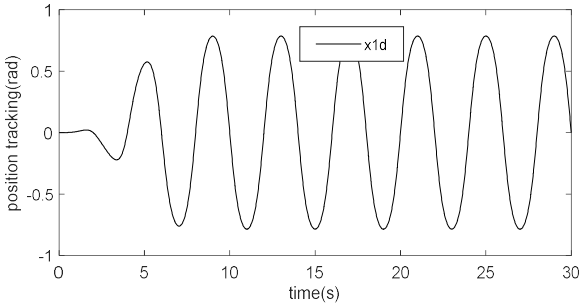

Fig. 4. The desired position trajectory in case 1

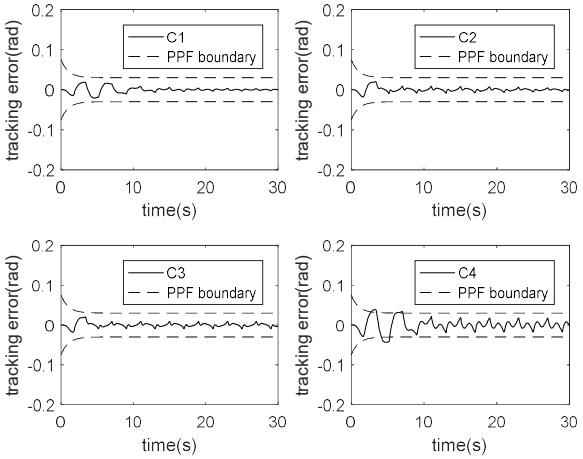

Fig. 5. Tracking errors of the compared controllers in case 1

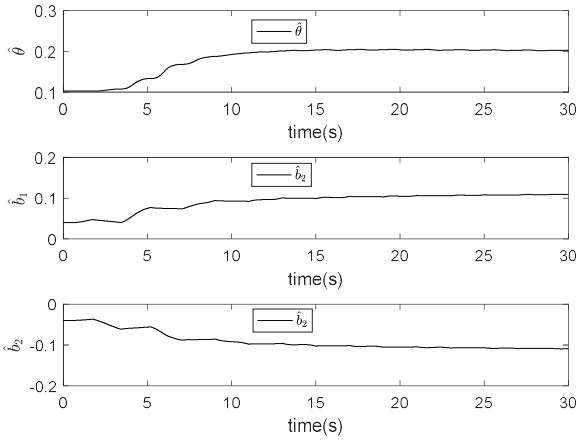

Fig. 6. Parameters estimations in case 1

TABLE II
THE MAXIMUM TRACKING ERROR AT LAST TWO CYCLES IN CASE 1

C1/rad	C2/rad	C3/rad	C4/rad
0.0029	0.0053	0.0093	0.0179

Case 2:

The desired position trajectory is chosen as point-to-point command shown in Fig. 7. The maximum distance is 2rad, the maximum velocity is 3rad/s. The simulation step size is set as 0.0005s. The simulation results are shown in Fig. 7-9 and Table III.

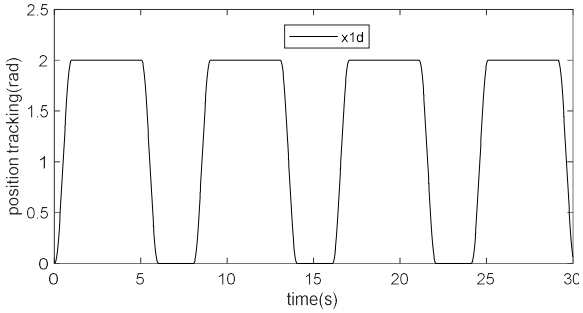

Fig. 7. The desired position trajectory in case 2

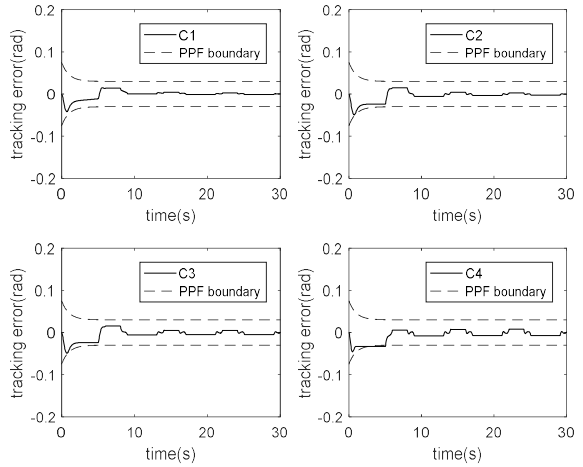

Fig. 8. Tracking errors of the compared controllers in case 2

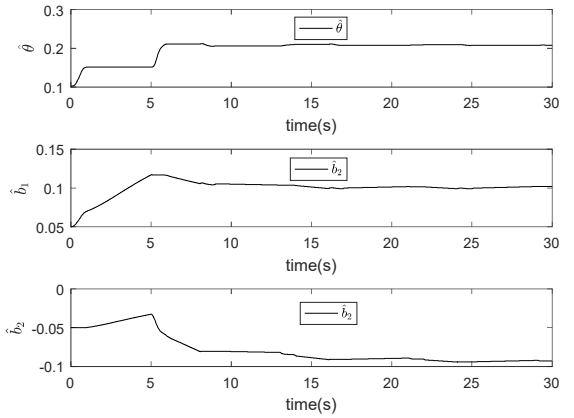

Fig. 9. Parameters estimations in case 2

TABLE III
THE MAXIMUM TRACKING ERROR AT LAST TWO CYCLES IN CASE 2

C1/rad	C2/rad	C3/rad	C4/rad
0.0036	0.0043	0.0055	0.0076

Analyzing Fig. 5, Fig. 8, Table II, and Table III, it can be seen that tracking error of C4 in the initial stage exceeds the prescribed performance function (PPF) boundary, while the transient and steady-state tracking errors of C1, C2, C3 always remain within the PPF boundary, which verifies the effectiveness of the prescribed performance design. Compared to C3, the steady-state tracking errors of C1 and C2 are smaller, which proves that the employed nonlinear robust term g_{r2} has well disturbance suppression effect. C1 can achieve the highest tracking accuracy, which thanks to the compensation for unknown dead-zone. It is easy to see from Fig. 7 and Fig. 9 that the estimations of dead-zone parameters converge well.

VI. Conclusion

The proposed novel controller is mainly used to solve the high-precision tracking control issue of motor servo system with input dead-zone. Firstly, rigorous theoretical analysis proves that the proposed controller can effectively compensate for dead-zone, achieve prescribed performance and asymptotic tracking. Secondly, through simulation comparison of four controllers, it was verified that all the technologies employed in the proposed controller can achieve the expected results. Finally, the novel control can be extended to various fields such as machine tools, electric manipulator, and so on.

References

[1] B. Yao, C. Hu, L. Lu, Q. Wang, "Adaptive robust precision motion control of a high-speed industrial gantry with cogging force compensations," *IEEE/ASME Transactions on Control Systems Technology,* vol. 19, no. 5, pp. 1149-1159, 2011.

[2] J. Yao, Z. Jiao, D. Ma, " Adaptive robust control of DC motors with extended state observer," *IEEE Transactions on Indurtrial Electronics,* vol. 61, no. 7, pp. 3630-3637, 2014.

[3] J. Hu, Y. Qiu, L. Liu, " High-order sliding-mode observer based output feedback adaptive robust control of a launching platform with backstepping," *International Journal of Control,* vol. 89, no. 10, pp. 2029-2039, 2016.

[4] J. Yao, Z. Jiao, D. Ma, "Extended-state-observer-based output feedback nonlinear robust control of hydraulic systems with backstepping", *IEEE Transactions on Indurtrial Electronics*, vol. 61, no. 11, pp. 6285-6293, 2014.

[5] Z. Dong, J. Ma, "Quasi-adaptive sliding mode motion control of hydraulic servo-mechanism with modeling uncertainty: a barrier function-based method," *IEEE Access,* vol. 8, pp. 143359-143365, 2020.

[6] Z. Dong, J. Yao, D. Ma, " Robust asymptotic tracking control of a chain of integrator nonlinear systems with input constraint and hysteresis nonlinearity," *Transactions of the Institute of Measurement and Control,* vol. 38, no. 12, pp. 1500-1508, 2016.

[7] G. Yang, J. Yao, Z. Dong, " Neuroadaptive learning algorithm for constrained nonlinear systems with disturbance rejection," *International Journal of Robust and Nonlinear Control,* vol. 32, no. 10, pp. 6127-6147, 2022.

[8] Hongyu Long, Yunlong He, Wei Xiang, Zhenqi Guan, Hao Tan, and Jianbo Yu, "Research on Short-term Wind Speed Prediction Based on Adaptive Hybrid Neural Network with Error Correction," IAENG International Journal of Computer Science, vol. 50, no.4, pp1290-1304, 2023

[9] Zhongda Tian, Xianwen Gao, and Dehua Wang, "The application research of fuzzy control with self-tuning of scaling factor in the energy saving control system of pumping unit," Engineering Letters*,* vol. 24, no. 2, pp187-194, 2016.

[10] Minoo Jafarlou, Omid Mahdi Ebadati E., and Hassan Naderi, "Improving Fuzzy-Logic based Map-Matching Method with Trajectory Stay-Point Detection," Lecture Notes in Engineering and Computer Science: Proceedings of The International MultiConference of Engineers and Computer Scientists 2023, 5-7 July, 2023, Hong Kong, pp48-57.

[11] Z. Zhang, J. Park, K. Zhang, J. Lu 'Adaptive control for a class of nonlinear time-delay systems with dead-zone input', *Journal of the Franklin Institute*, vol. 353, no. 17, pp. 4400-4421, 2016.

[12] G. Tao, P.V. Kokotovic, 'Adaptive control of plants with unknown dead-zones', *IEEE Transactions on Automatic Control*, vol. 39, no. 1, pp. 59-68, 1994.

[13] W. Deng, J. Yao, D. Ma, 'Robust adaptive precision motion control of hydraulic actuators with valve dead-zone compensation', *ISA Transaction*, vol. 70, pp. 269-278, 2017.

[14] C. P. Bechlioulis, G. A. Rovithakis, 'Adaptive control with guaranteed transient and steady state tracking error bounds for strict feedback systems', *Automatica*, vol. 45, no. 2, pp. 532-538, 2009.

[15] Z. Xu, X. Zhou, Z. Dong, X. Hu, C. Sun, H. Shen, " Observer-based prescribed performance adaptive neural output feedback control for

full-state-constrained nonlinear systems with input saturation," *Chaos Solitons & Fractal,* vol. 173, 2023.

[16] J. Na, Q. Chen, X. Ren, and Y. Guo, 'Adaptive prescribed performance motion control of servo mechanisms with friction compensation', *IEEE Transactions on Indurtrial Electronics*, vol. 61, no. 1, pp. 486-494, 2014.

[17] Decai Liu, Xinyu Ouyang, Nannan Zhao, and Yu Luo, "Adaptive Event-triggered Control with Prescribed Performance for Nonlinear System with Full-state Constraints," IAENG International Journal of Applied Mathematics, vol. 54, no. 3, pp390-397, 2024

[18] Z. Dong, J. Ma, J. Yao, " Barrier function-based asymptotic tracking control of uncertain nonlinear systems with multiple states constraints," *IEEE Access*, vol. 8, pp. 14917-14927, 2020.

[19] M. Krstic, I. Kanellakopoulos, P. V. Kokotovic, 'Nonlinear and adaptive control design', New York: Wiley, 1995.